Supporting Information

Highly Efficient and Selective Oxidation of Benzyl Alcohol by WO_4^{2-} Catalyst Immobilized by a Phosphonium-Containing Porous Aromatic Framework

Bingxin You [1], Zeliang Cheng [2], Yuyang Tian [2], Shaolei Wang [2,*] and Baolin Wang [2,*]

[1] Center of Disease Immunity and Intervention, College of Medicine, Lishui University, Lishui 323000, China; youbx634@nenu.edu.cn
[2] Key Laboratory of Polyoxometalate and Reticular Material Chemistry of the Ministry of Education, Faculty of Chemistry, Northeast Normal University, Changchun 130024, China; chengzl968@nenu.edu.cn (Z.C.); tianyy100@nenu.edu.cn (Y.T.)
* Correspondence: wangsl030@nenu.edu.cn (S.W.); wangbl296@nenu.edu.cn (B.W.)

Characterization details

Fourier transform infrared spectroscopy (FT-IR) was performed on a Nicolet IS50 FT-IR spectrometer (Thermo Scientific, Waltham, MA, USA), and PAF pellets were prepared by adding KBr. The ^{13}C and ^{31}P CP/MAS solid-state NMR spectra of PAFs were measured using a Bruker Advance III model 400 MHz NMR spectrometer (Bruker, Karlsruhe, Germany) at a MAS rate of 5 kHz. The morphology of the PAFs was characterized using a field emission scanning electron microscope (FE-SEM, SU-8010, Hitachi, Tokyo, Japan). Transmission electron microscopy (TEM) was performed using a JEOL JEM-2100PLUS TEM (Tokyo, Japan) at an acceleration voltage of 200 kV, and samples were prepared by dropping a suspension of PAFs suspended in ethanol onto the microgrid. PXRD measurements were carried out on a Rigaku Smart-Lab X-ray diffractometer (Tokyo, Japan) with Cu-Kα radiation (40 kV, 30 mA, $\lambda = 1.5418$ Å) and a scanning step of 0.01 °. The elemental analysis (for P and W) was performed using an inductively coupled plasma atomic emission spectrometer (ICP-AES) on a LEEMAN Prodigy (Hudson, NH, USA). Thermogravimetric analysis (TGA) was performed using a METTLER-TOLEDO TGA/DSC 3+ analyzer (Greifensee, Switzerland) under an air atmosphere at a heating rate of 10 °C min^{-1}. A Quantachrome Autosorb-iQ2 analyzer (Boynton Beach, FL, USA) was used to analyze the specific surface area and pore structure with N_2 as the probe molecule at 77 K. The water contact angle was detected using a CA-100C&D contact angle meter. Before the test, the samples were degassed at 100 °C for 10 h. Gas chromatography mass spectrometry (GC-MS) analysis was employed for determining the catalytic reaction products using a Thermo Scientific Trace 1310-ISQ 7000 system (Waltham, MA, USA). Ultra-pure helium was used as the carrier gas, and the temperatures for the injection port and detector were both 250 °C.

Chemicals

All chemicals used in the experiments were of analytical grade and were used without further purification unless otherwise specified. All (dehydrated) solvents, dichloromethane (DCM), tetrahydrofuran (THF), and *N*, *N*-dimethylformamide (DMF) were purchased from Beijing InnoChem Science & Technology Co., Ltd (Beijing, China). All chemicals, 4,4′-dibromobiphenyl, phosphorus trichloride (PCl_3), 2.50 M *n*-butyllithium (2.50 M *n*-BuLi), iodomethane (CH_3I), sodium tungstate dihydrate (Na_2WO_4 $2H_2O$), benzyl alcohol and their derivatives, were purchased from Beijing InnoChem Science & Technology Co., Ltd.; Bis(1,5-cyclooctadiene)nickel(0) [$Ni(cod)_2$], 1,5-cyclooctadiene (cod), and 2,2′-bipyridine were purchased from TCI Shanghai; 30% hydrogen peroxide (30% H_2O_2), sodium hydrogen sulfate ($NaHSO_4$), tartaric acid, and *p*-toluenesulfonic acid (TsOH) were purchased from local drug suppliers.

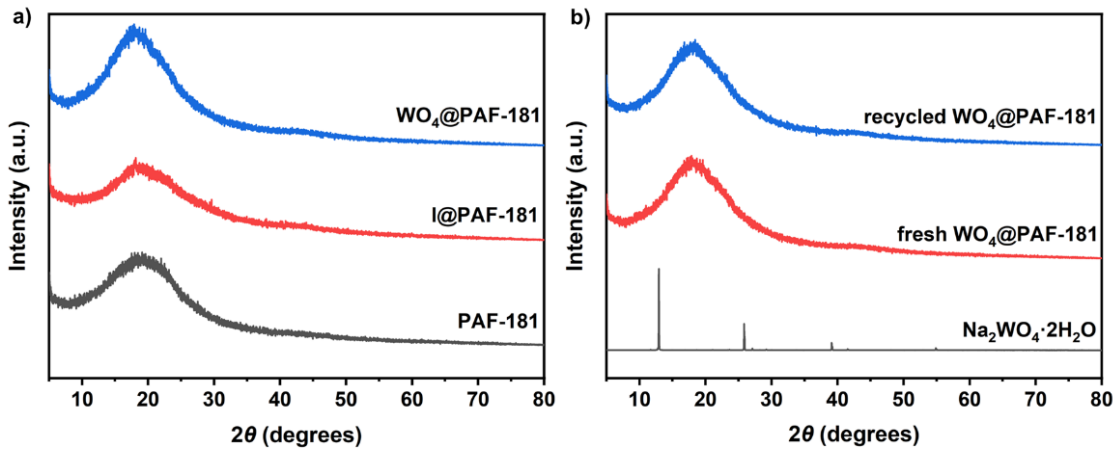

Figure S1. Experimental PXRD patterns of PAF-181, I@PAF-181, and WO_4@PAF-181 (a); $Na_2WO_4 \cdot 2H_2O$, fresh WO_4@PAF-181, and recycled WO_4@PAF-181 (b).

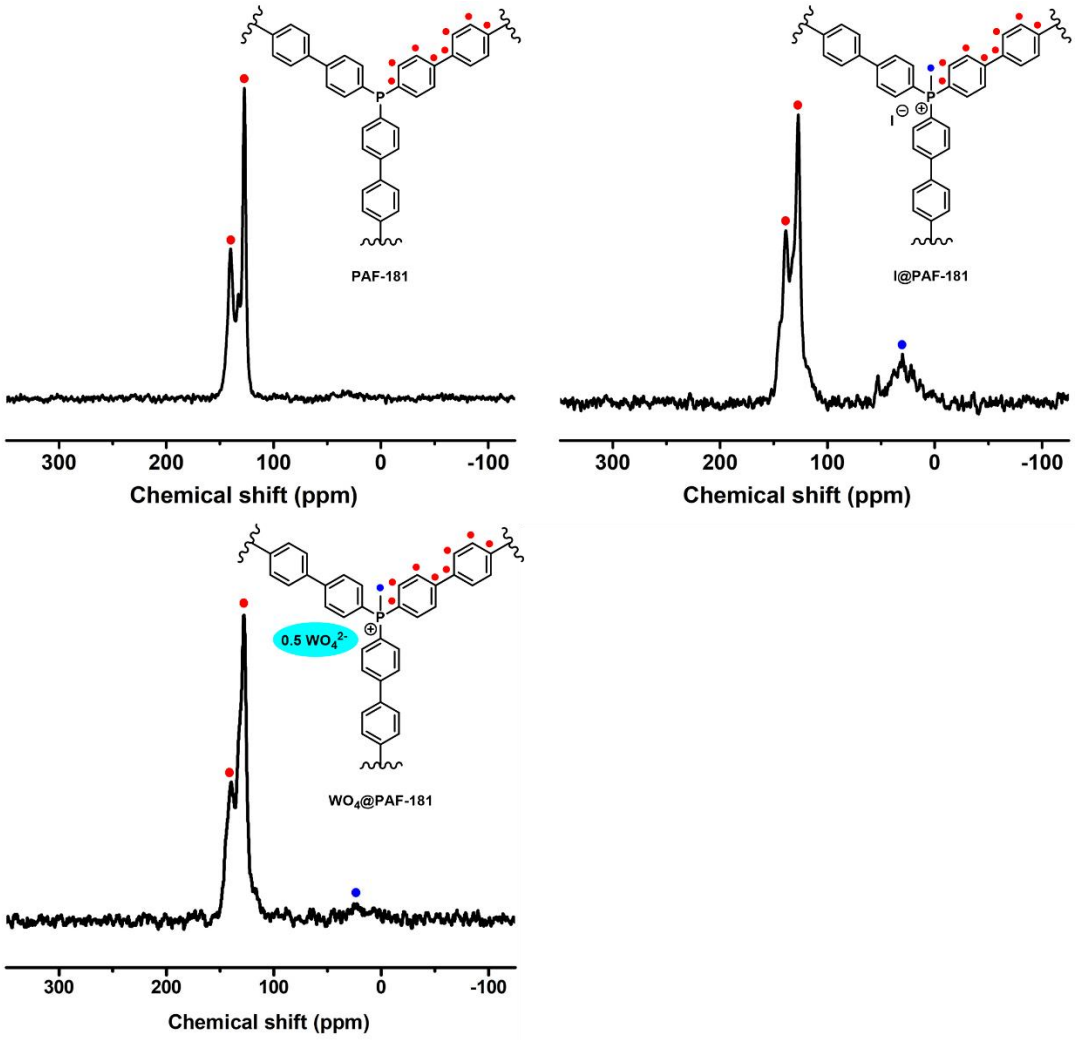

Figure S2. ^{13}C CP/MAS solid-state NMR spectra of PAF-181, I@PAF-181, and WO_4@PAF-181.

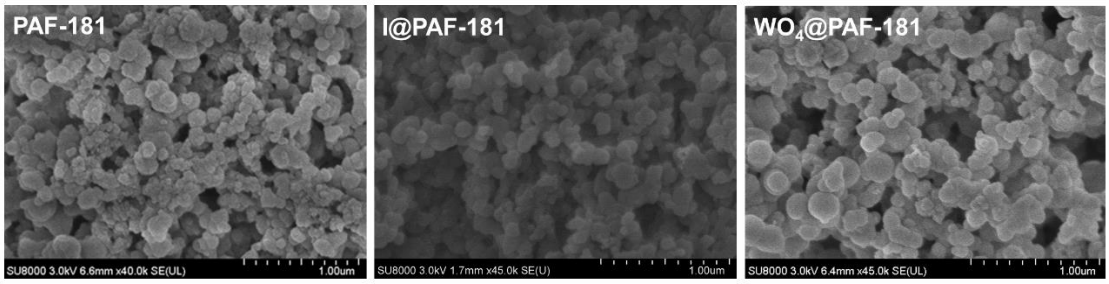

Figure S3. SEM images of PAF-181, I@PAF-181, and WO_4@PAF-181.

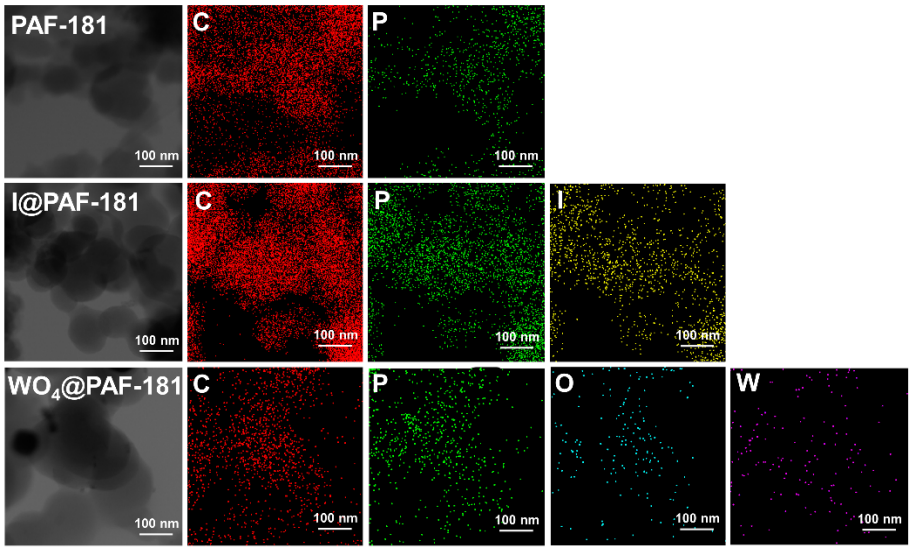

Figure S4. TEM-EDX mapping images of PAF-181, I@PAF-181, and WO_4@PAF-181.

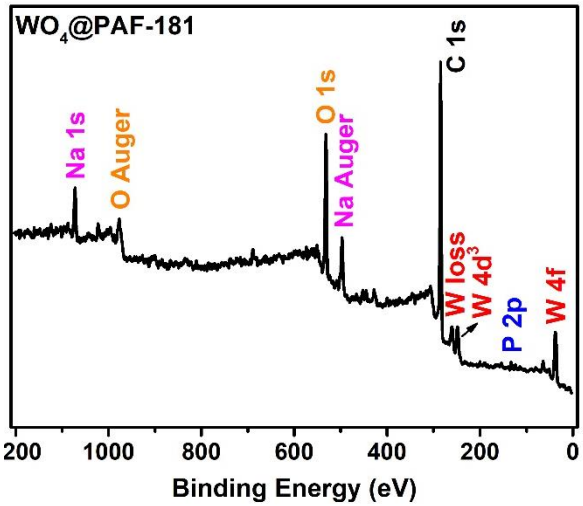

Figure S5. XPS survey scan of WO_4@PAF-181.

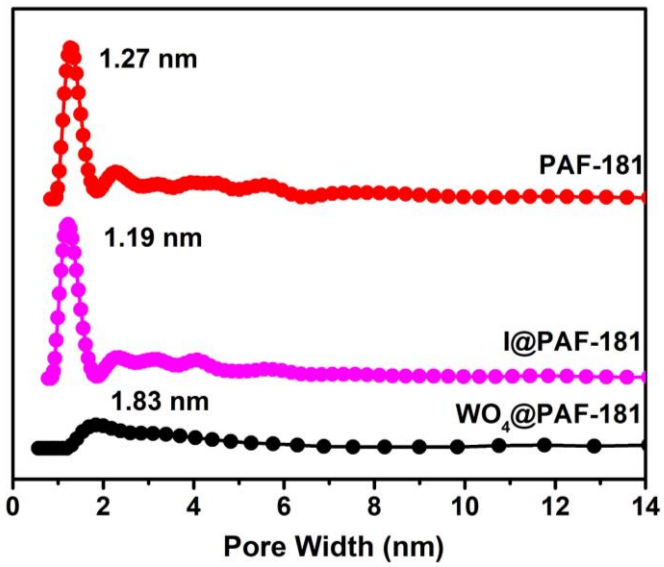

Figure S6. Pore size distributions of PAF-181, I@PAF-181, and WO_4@PAF-181.

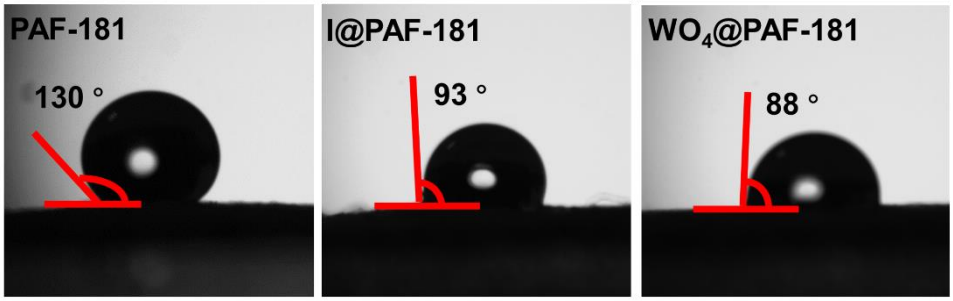

Figure S7. The water contact angles of PAF-181, I@PAF-181, and WO_4@PAF-181.

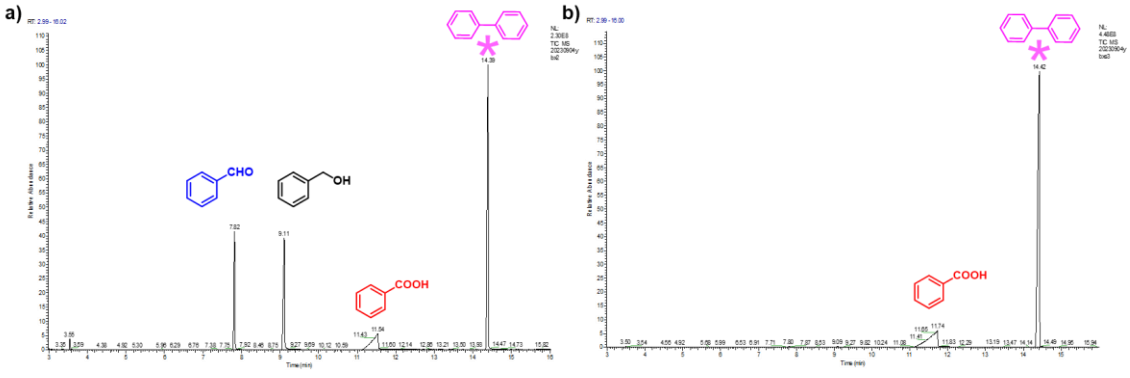

Figure S8. GC spectrum of the standard mixed solution of ethyl acetate in equimolar amounts of benzyl alcohol, benzaldehyde, benzoic acid, and biphenyl (internal standard) (a); GC spectrum for the optimal reaction conditions (b).

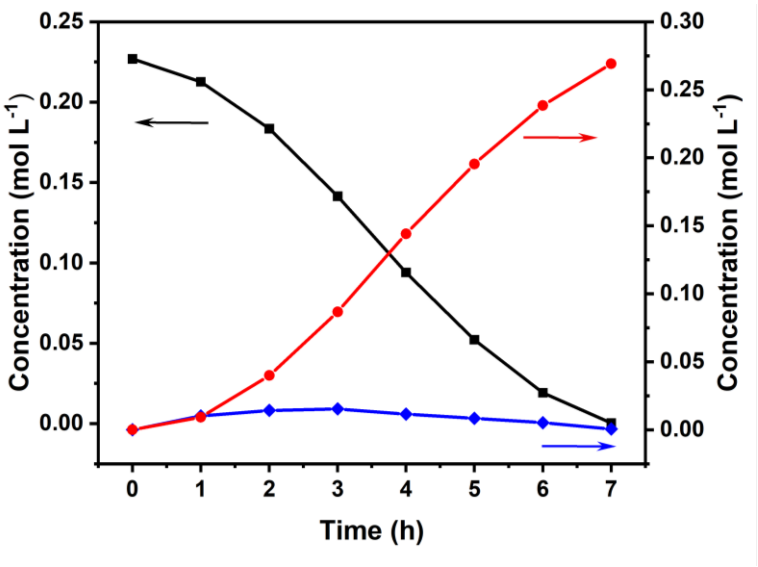

Figure S9. Plot of unconverted amount of benzyl alcohol and yield of benzaldehyde and benzoic acid vs. time during the oxidation of benzyl alcohol under optimal reaction conditions.

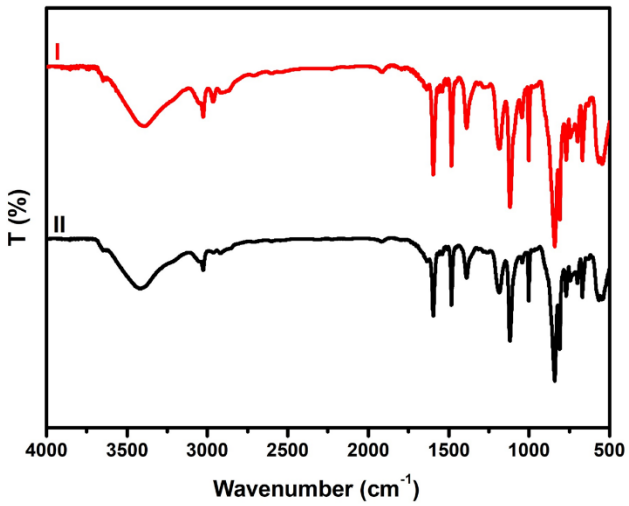

Figure S10. FT-IR spectra of fresh WO_4@PAF-184 (I) and recycled WO_4@PAF-184 (II).

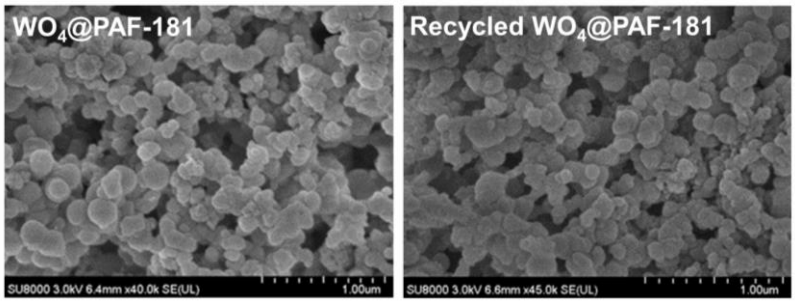

Figure S11. SEM images of fresh WO_4@PAF-181 and recycled WO_4@PAF-181.

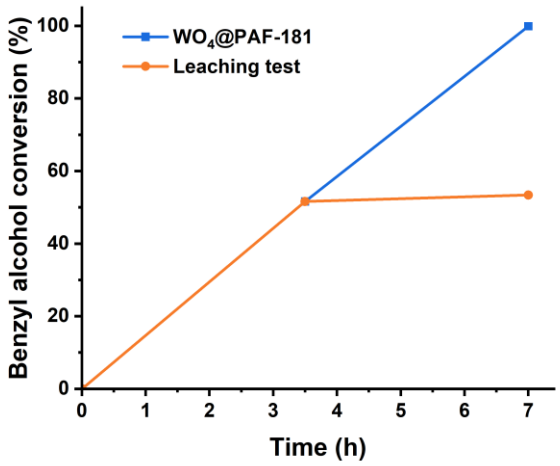

Figure S12. Plot of benzyl alcohol conversion vs. time for the oxidation of benzyl alcohol, under the reaction conditions of entry 11, Table 1, in the presence of WO_4@PAF-181 (blue curve) and after filtering off the catalyst WO_4@PAF-181 after 3.5 h reaction time (orange curve).

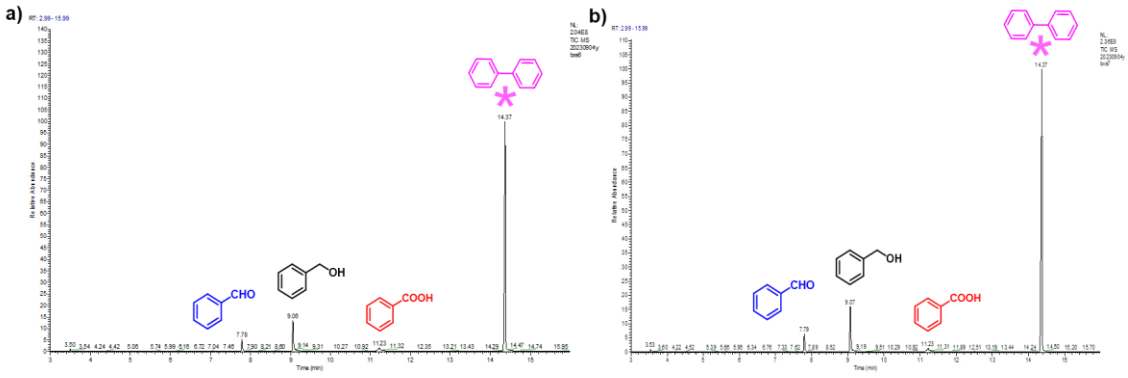

Figure S13. GC spectra of the filtrate at 3.5 h with WO_4@PAF-181 (a) and at 7 h without WO_4@PAF-181 (b) during the hot filtration test.

Table S1. ICP-AES test results for the P and W content of PAF-181, fresh WO_4@PAF-181, recycled WO_4@PAF-181 (red font), and the filtrate after filtering off the catalyst WO_4@PAF-181 during the hot filtration test.

	PAF-181	WO_4@PAF-181	WO_4@PAF-181	filtrate
P	5.8 wt%	4.1 wt%	4.0 wt%	-
W	-	14.1 wt%	13.5 wt%	0 wt%

Table S2. Characteristics of pores in PAF-181, I@PAF-181, and WO_4@PAF-181 (calculated from their N_2 adsorption–desorption isotherms at 77 K using quenched solid density functional theory).

	PAF-181	I@-PAF-181	WO_4@PAF-181
BET specific surface area (m^2/g)	1029	579	45
micropore area (m^2/g)	660	286	6
external surface area (m^2/g)	369	293	39
total pore volume (cc/g)	0.88	0.51	0.27
micropore volume (cc/g)	0.29	0.13	0.01
pore volume (cc/g)	0.73	0.44	0.11
mean pore diameter (nm)	3.44	3.54	24.1
main pore width (nm)	1.27	1.19	1.83

NMR Spectra

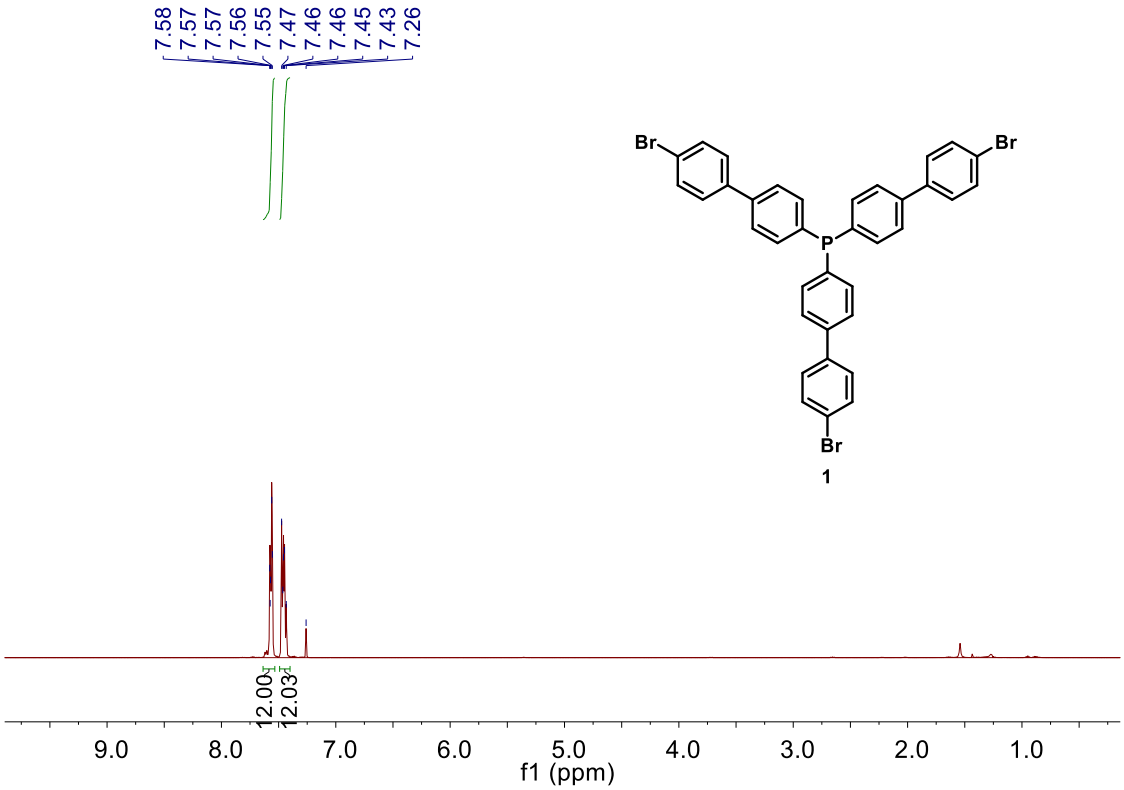
7.58
7.57
7.57
7.56
7.55
7.47
7.46
7.46
7.45
7.43
7.26
Br
Br
P
Br
1
12.00
12.03
9.0
8.0
7.0
6.0
5.0
4.0
3.0
2.0
1.0
f1 (ppm)

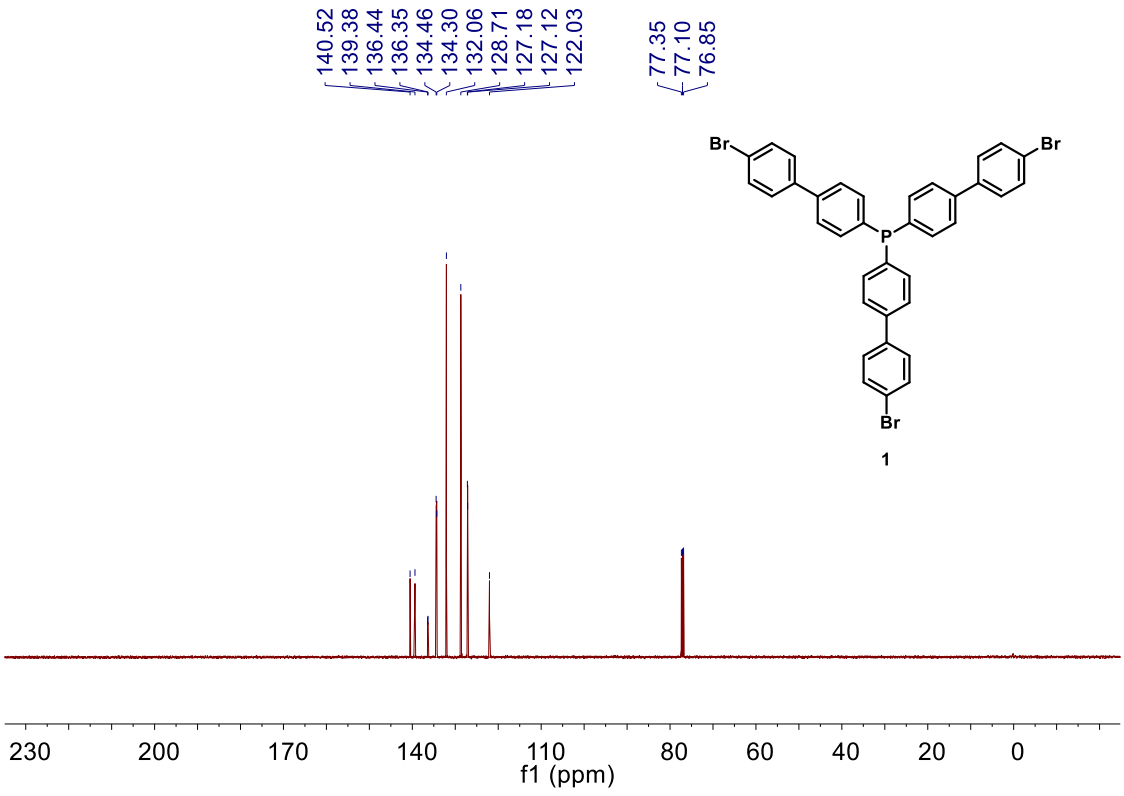
140.52
139.38
136.44
136.35
134.46
134.30
132.06
128.71
127.18
127.12
122.03
77.35
77.10
76.85
Br
Br
P
Br
1
230
200
170
140
110
80
60
40
20
0
f1 (ppm)

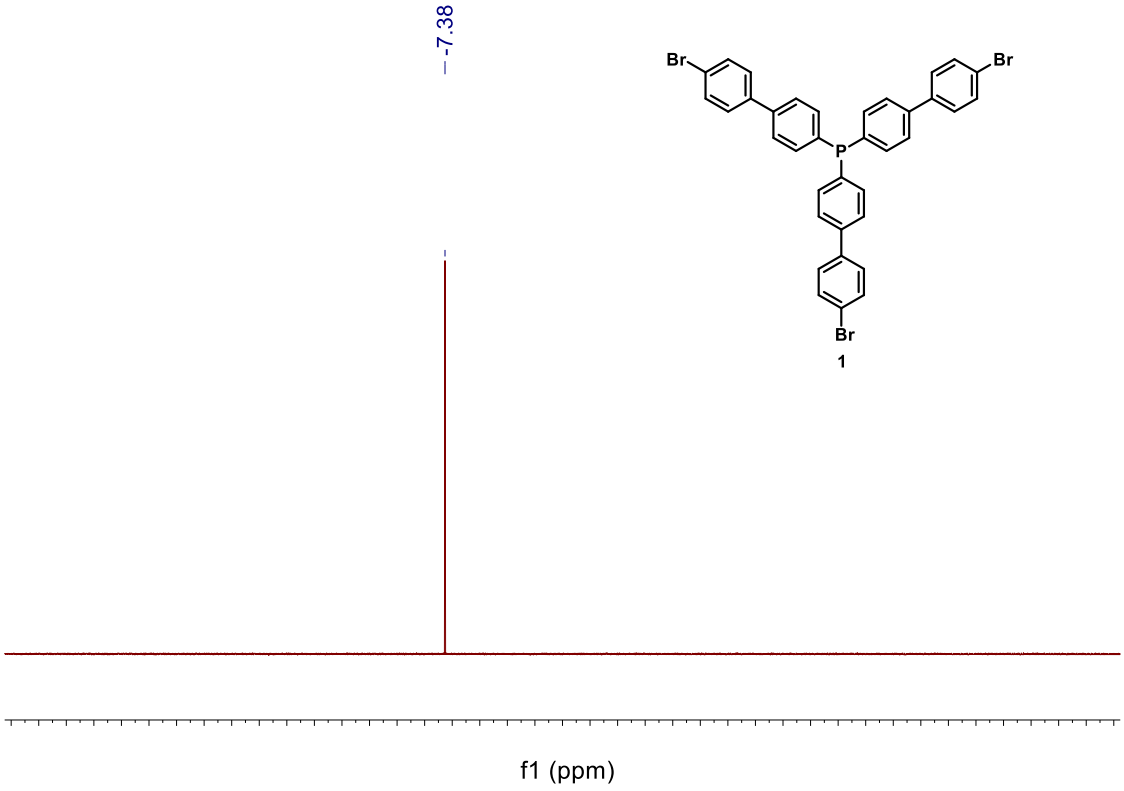
-7.38
Br
Br
P
Br
1
f1 (ppm)

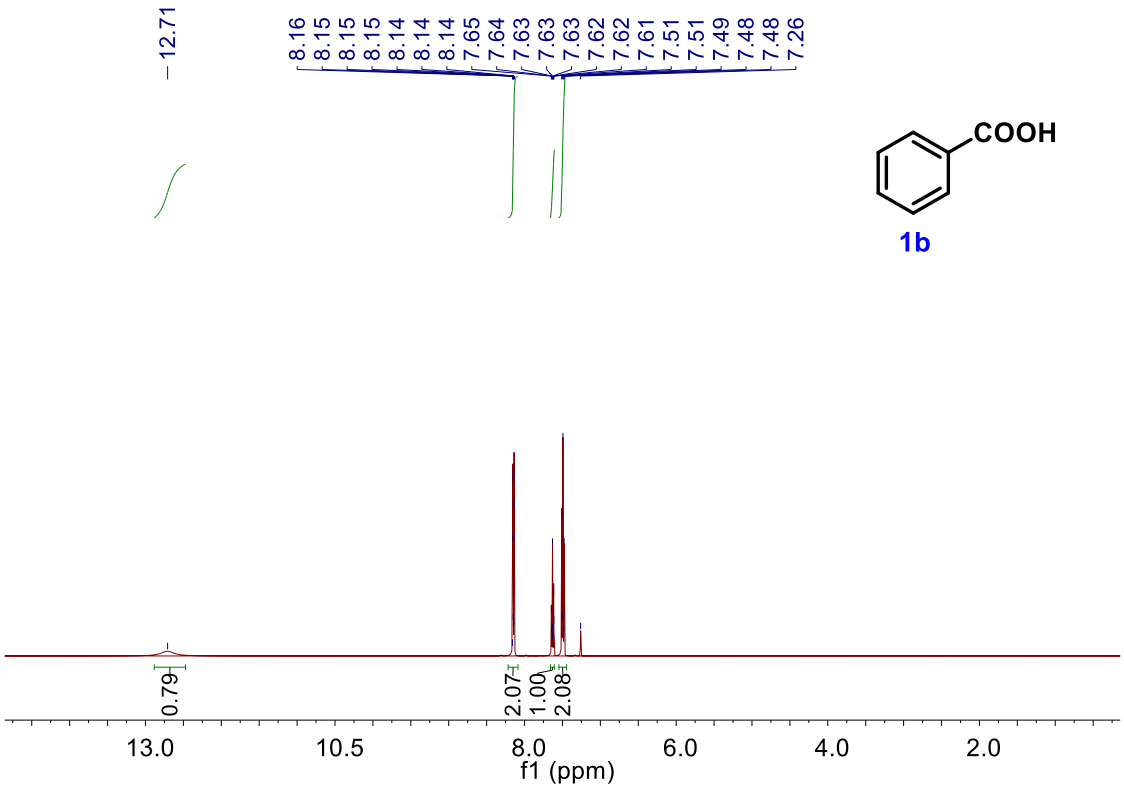
12.71
8.16
8.15
8.15
8.15
8.14
8.14
8.14
7.65
7.64
7.63
7.63
7.63
7.62
7.62
7.61
7.51
7.51
7.49
7.48
7.48
7.26
COOH
1b
0.79
2.07
1.00
2.08
13.0
10.5
8.0
6.0
4.0
2.0
f1 (ppm)

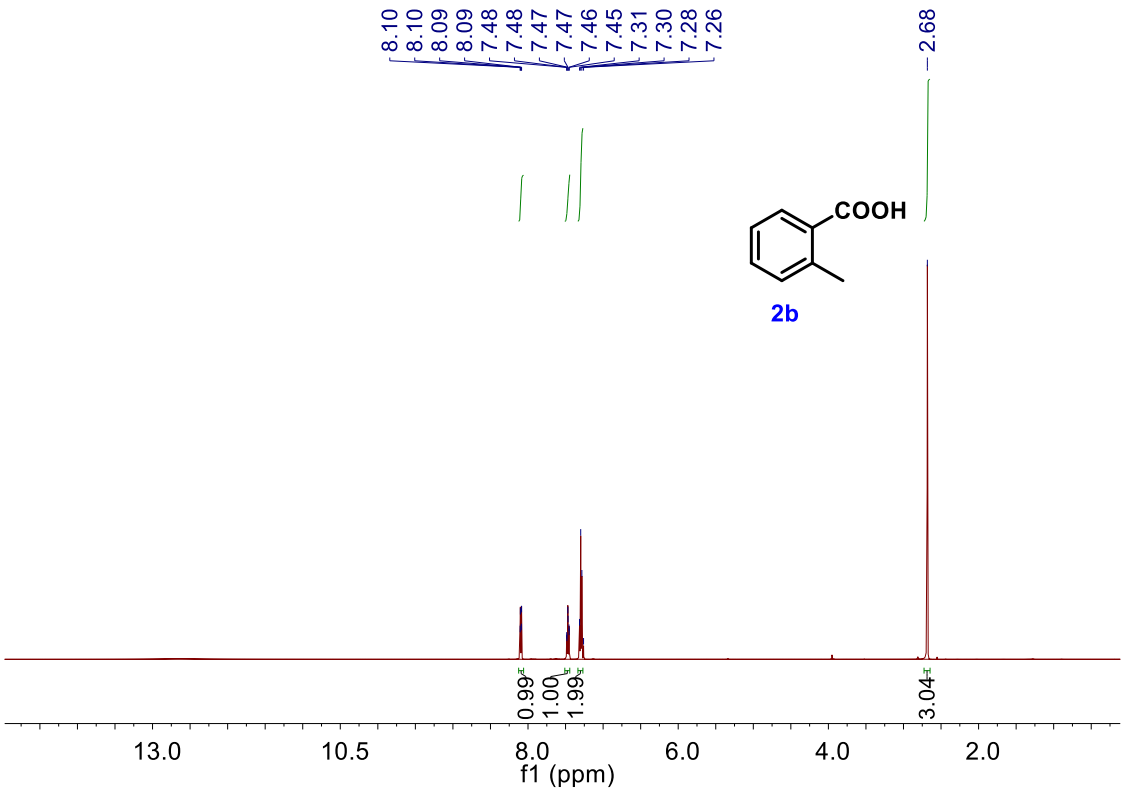
8.10
8.10
8.09
8.09
7.48
7.48
7.47
7.47
7.46
7.45
7.31
7.30
7.28
7.26
2.68
COOH
2b
0.99
1.00
1.99
3.04
13.0
10.5
8.0
6.0
4.0
2.0
f1 (ppm)

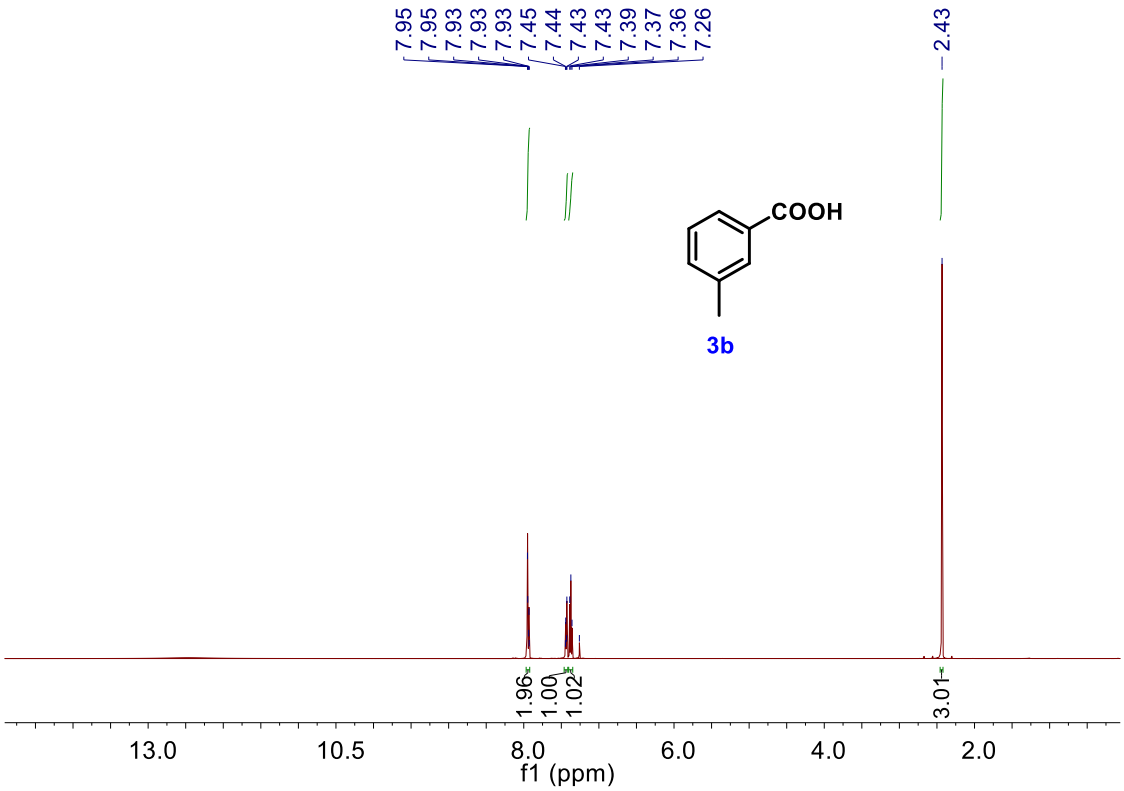
7.95
7.95
7.93
7.93
7.93
7.45
7.44
7.43
7.43
7.39
7.37
7.36
7.26
2.43
COOH
3b
1.96
1.00
1.02
3.01
13.0
10.5
8.0
6.0
4.0
2.0
f1 (ppm)

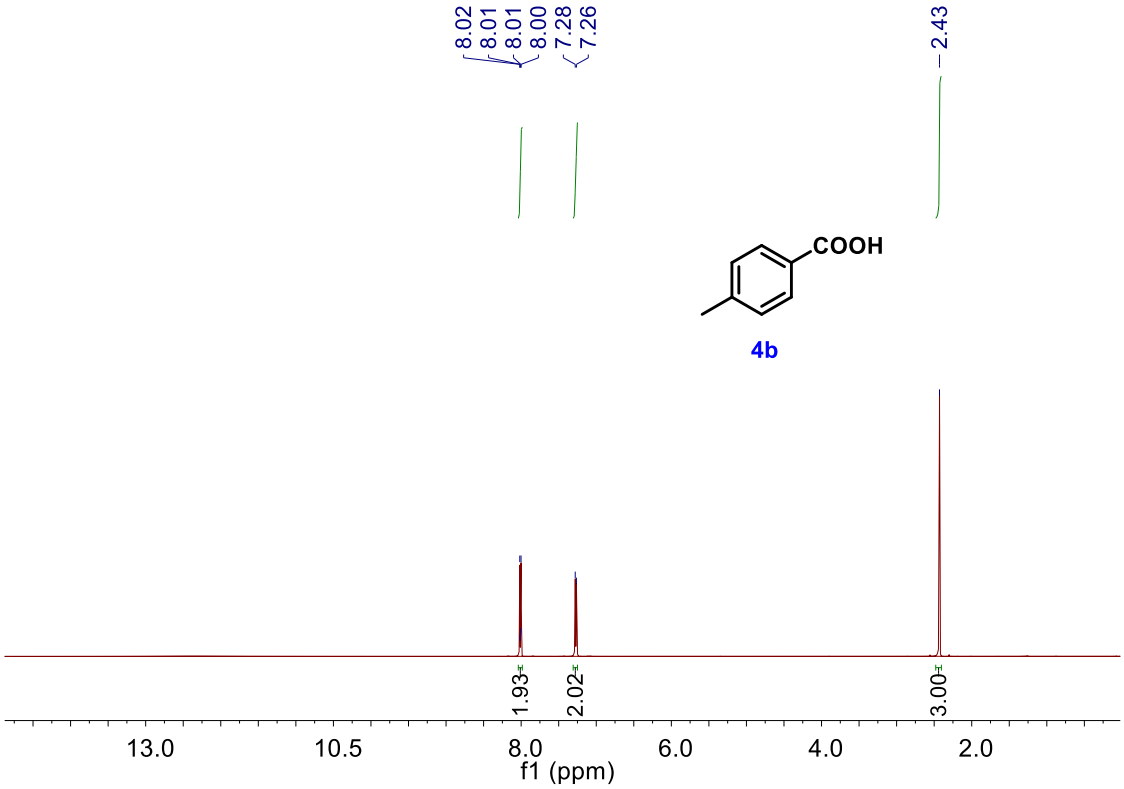
8.02
8.01
8.01
8.00
7.28
7.26
2.43
COOH
4b
1.93
2.02
3.00
13.0
10.5
8.0
6.0
4.0
2.0
f1 (ppm)

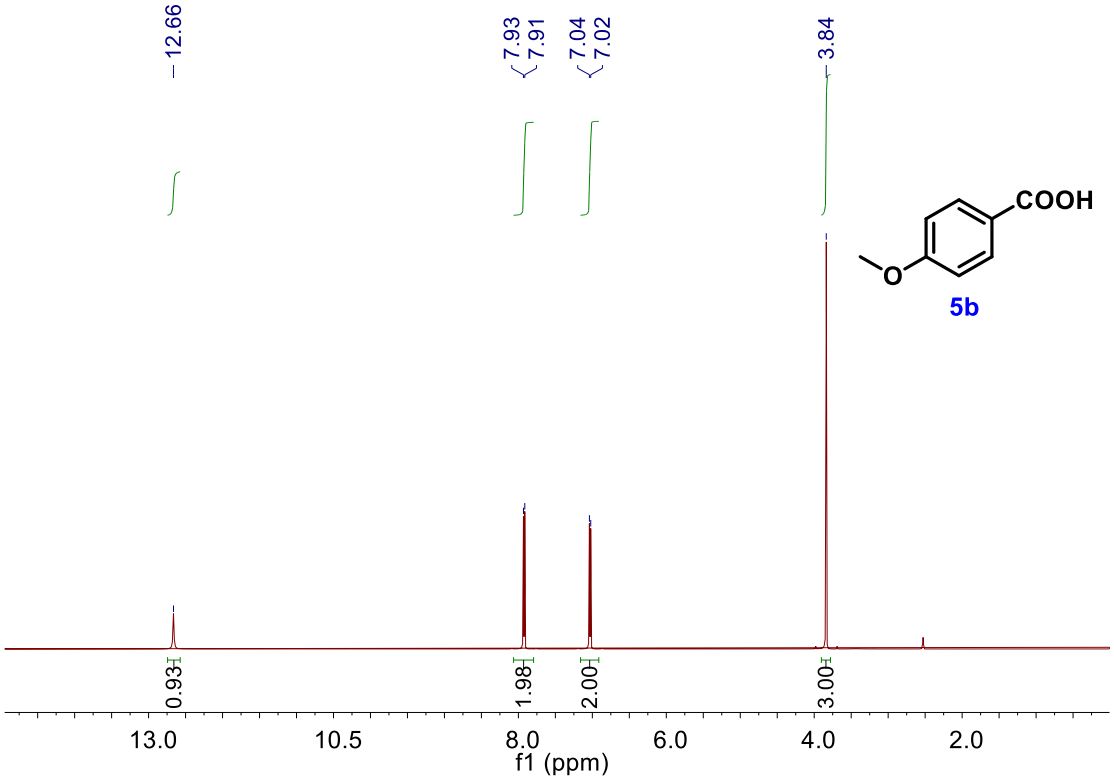
12.66
7.93
7.91
7.04
7.02
3.84
COOH
O
5b
0.93
1.98
2.00
3.00
13.0
10.5
8.0
6.0
4.0
2.0
f1 (ppm)

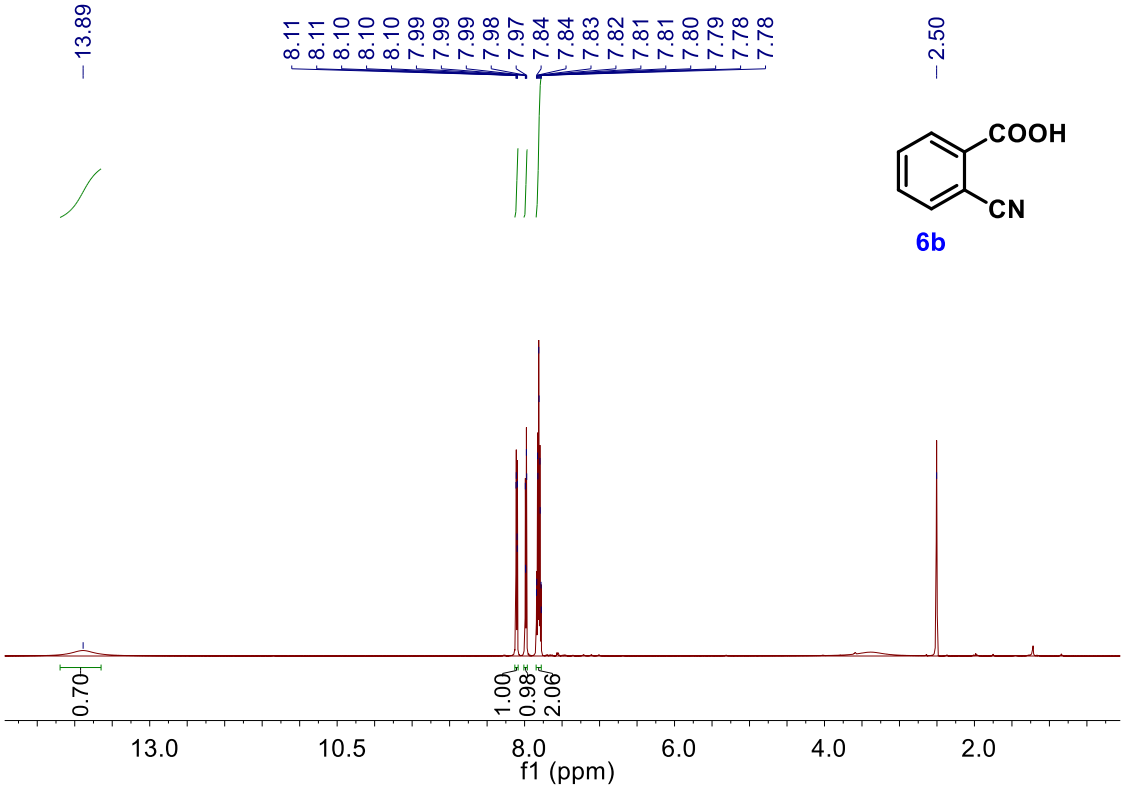
13.89
8.11
8.11
8.10
8.10
8.10
7.99
7.99
7.99
7.98
7.97
7.84
7.84
7.83
7.82
7.81
7.81
7.80
7.79
7.78
7.78
2.50
COOH
CN
6b
0.70
1.00
0.98
2.06
13.0
10.5
8.0
6.0
4.0
2.0
f1 (ppm)

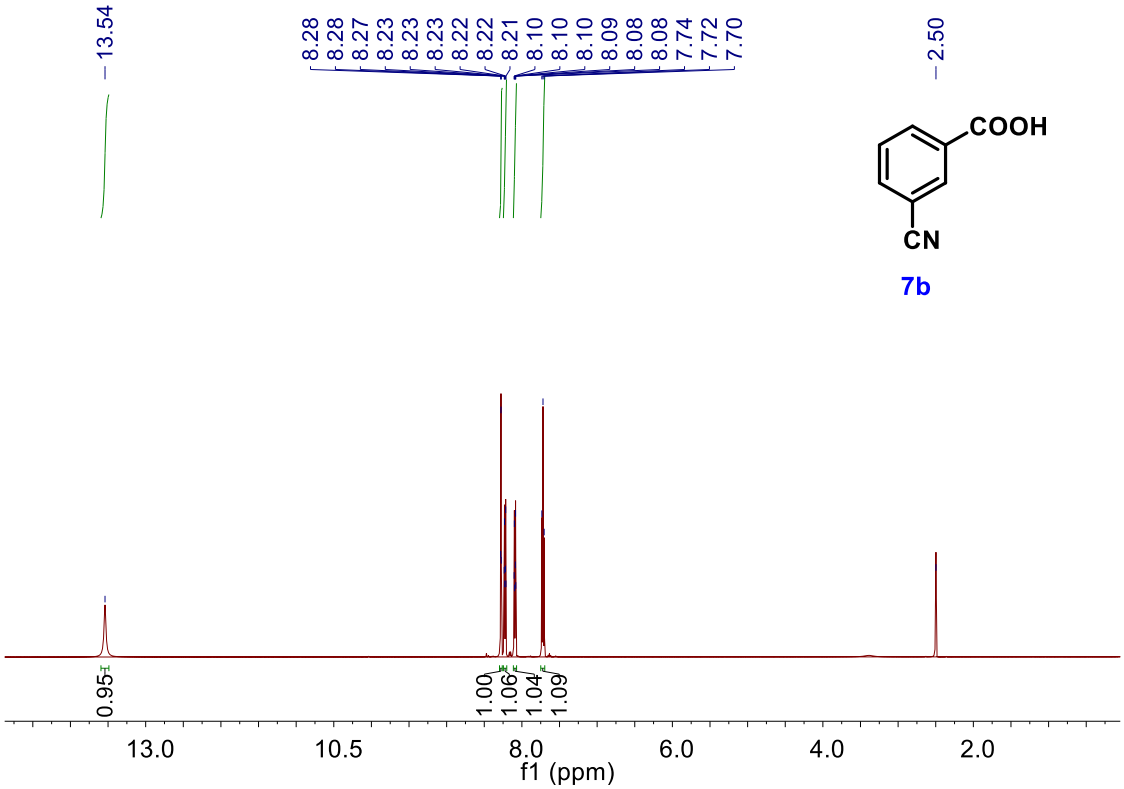
13.54
8.28
8.28
8.27
8.23
8.23
8.23
8.22
8.22
8.21
8.10
8.10
8.10
8.09
8.08
8.08
7.74
7.72
7.70
2.50
COOH
CN
7b
0.95
1.00
1.06
1.04
1.09
13.0
10.5
8.0
6.0
4.0
2.0
f1 (ppm)

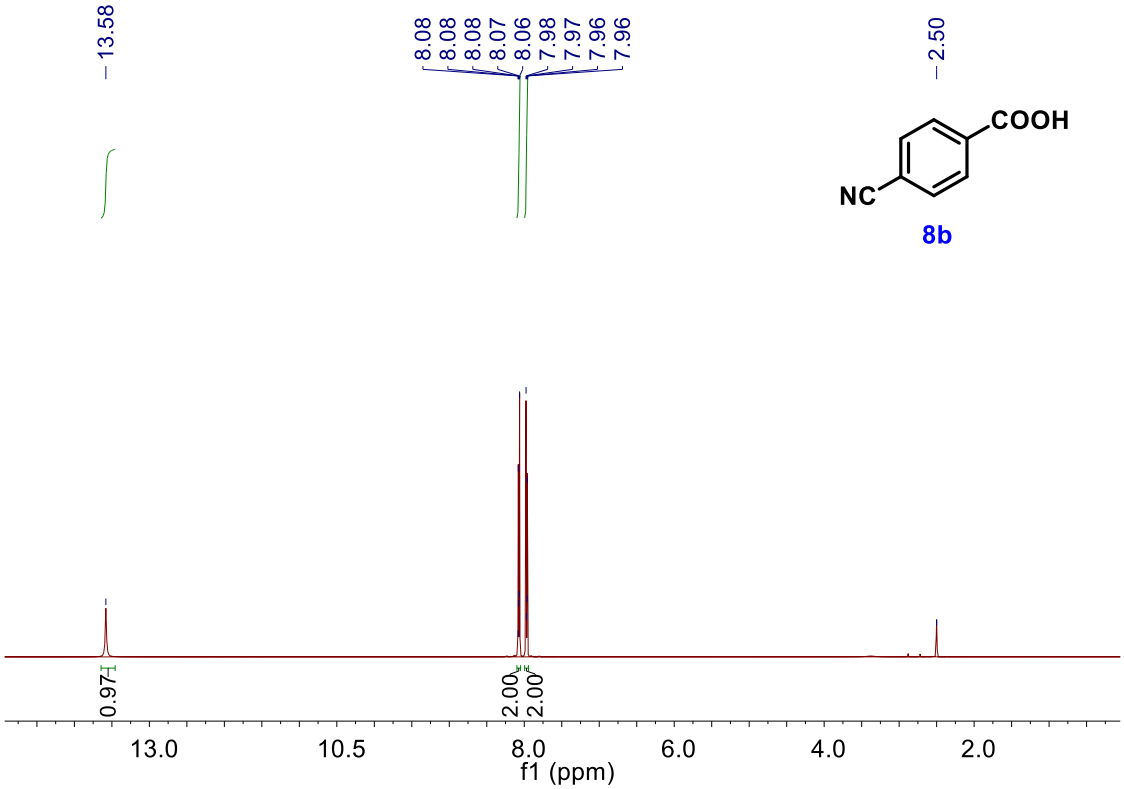
13.58
8.08
8.08
8.08
8.07
8.06
7.98
7.97
7.96
7.96
2.50
COOH
NC
8b
0.97
2.00
2.00
13.0
10.5
8.0
6.0
4.0
2.0
f1 (ppm)

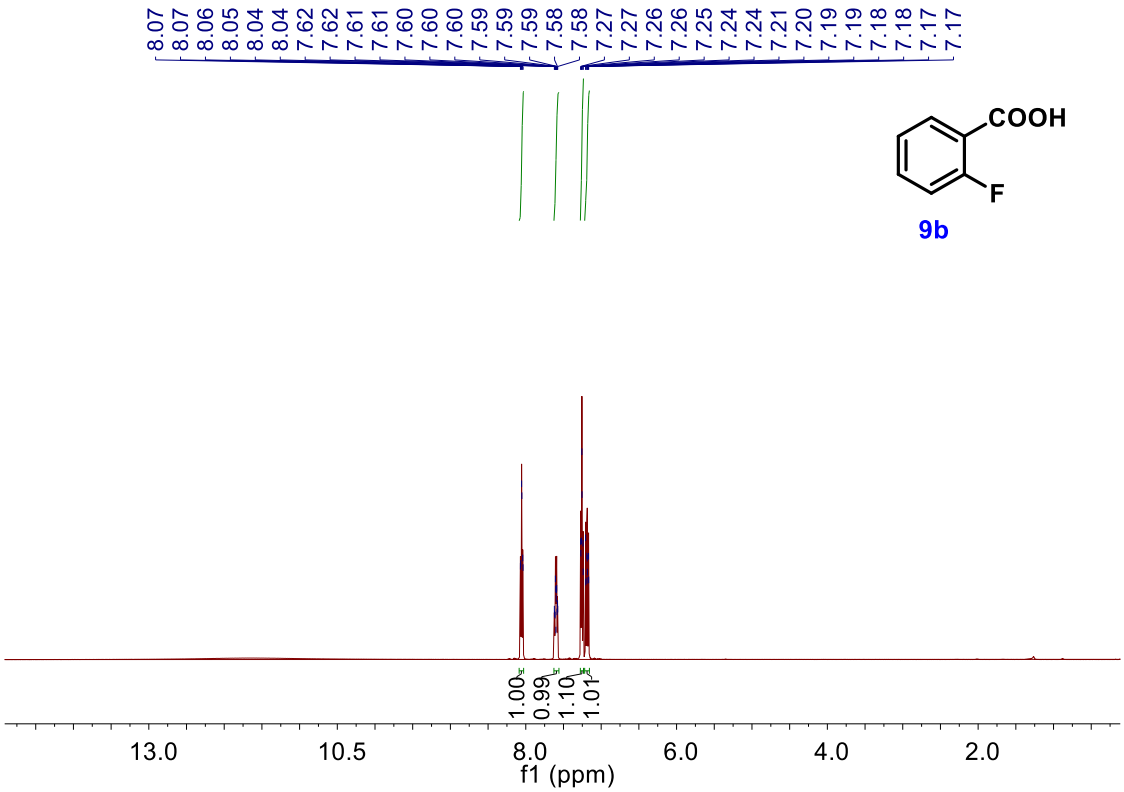
8.07
8.07
8.06
8.05
8.04
8.04
7.62
7.62
7.61
7.61
7.60
7.60
7.60
7.59
7.59
7.59
7.58
7.58
7.27
7.27
7.26
7.26
7.25
7.24
7.24
7.21
7.20
7.19
7.19
7.18
7.18
7.17
7.17
COOH
F
9b
1.00
0.99
1.10
1.01
13.0
10.5
8.0
6.0
4.0
2.0
f1 (ppm)

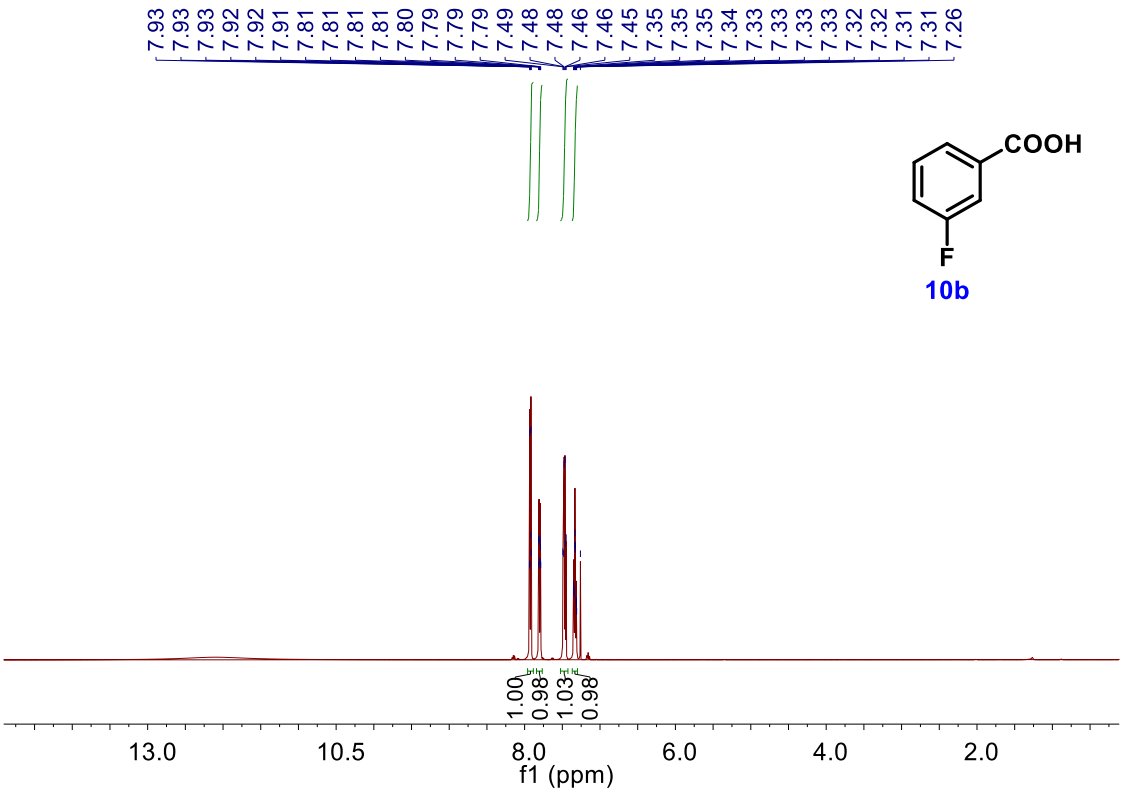
7.93
7.93
7.93
7.92
7.92
7.91
7.81
7.81
7.81
7.81
7.80
7.79
7.79
7.79
7.49
7.48
7.48
7.46
7.46
7.45
7.35
7.35
7.35
7.34
7.33
7.33
7.33
7.33
7.32
7.32
7.31
7.31
7.26
COOH
F
10b
1.00
0.98
1.03
0.98
13.0
10.5
8.0
6.0
4.0
2.0
f1 (ppm)

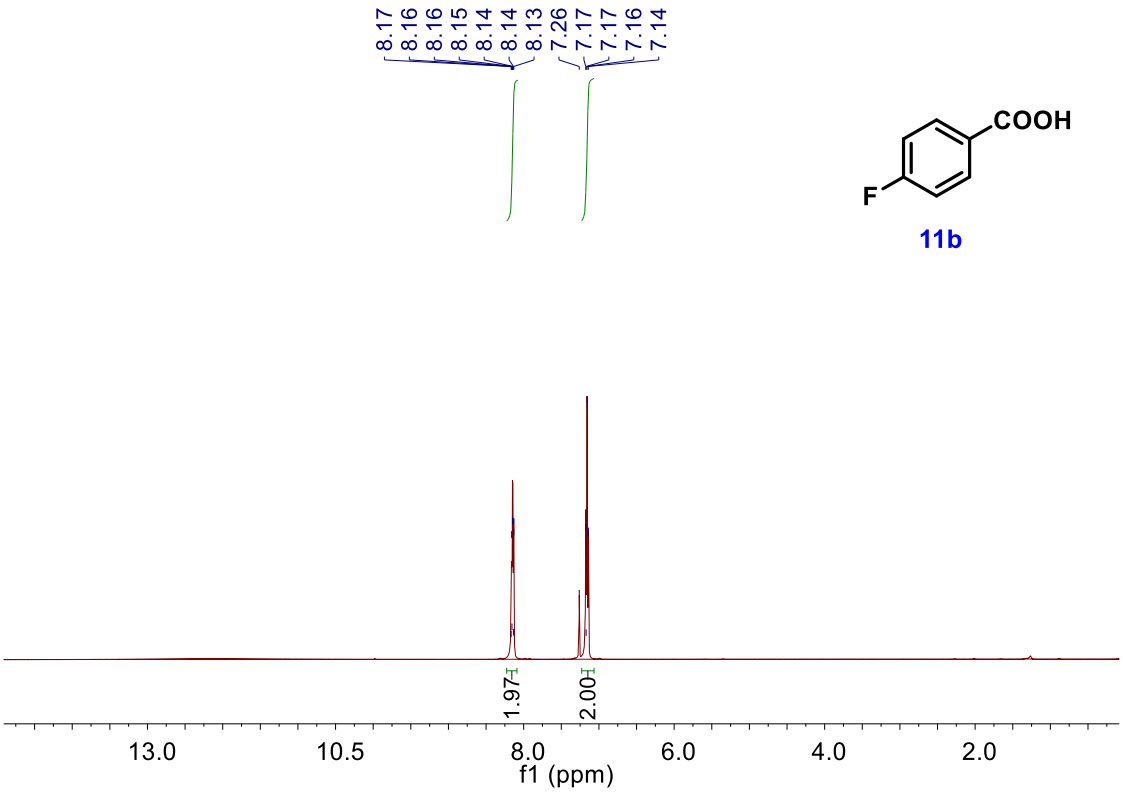
8.17
8.16
8.16
8.15
8.14
8.14
8.13
7.26
7.17
7.17
7.16
7.14
COOH
F
11b
1.97
2.00
13.0
10.5
8.0
6.0
4.0
2.0
f1 (ppm)

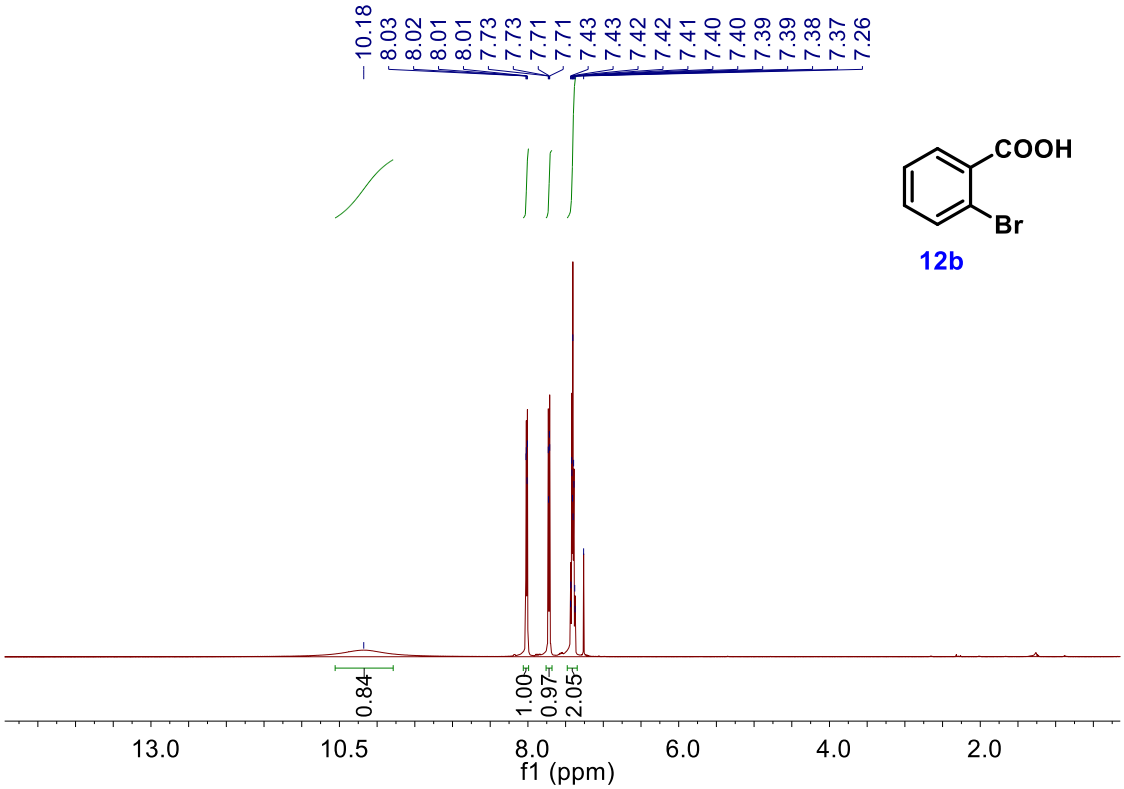
10.18
8.03
8.02
8.01
8.01
7.73
7.73
7.71
7.71
7.43
7.43
7.42
7.42
7.41
7.40
7.40
7.39
7.39
7.38
7.37
7.26
COOH
Br
12b
0.84
1.00
0.97
2.05
13.0
10.5
8.0
6.0
4.0
2.0
f1 (ppm)

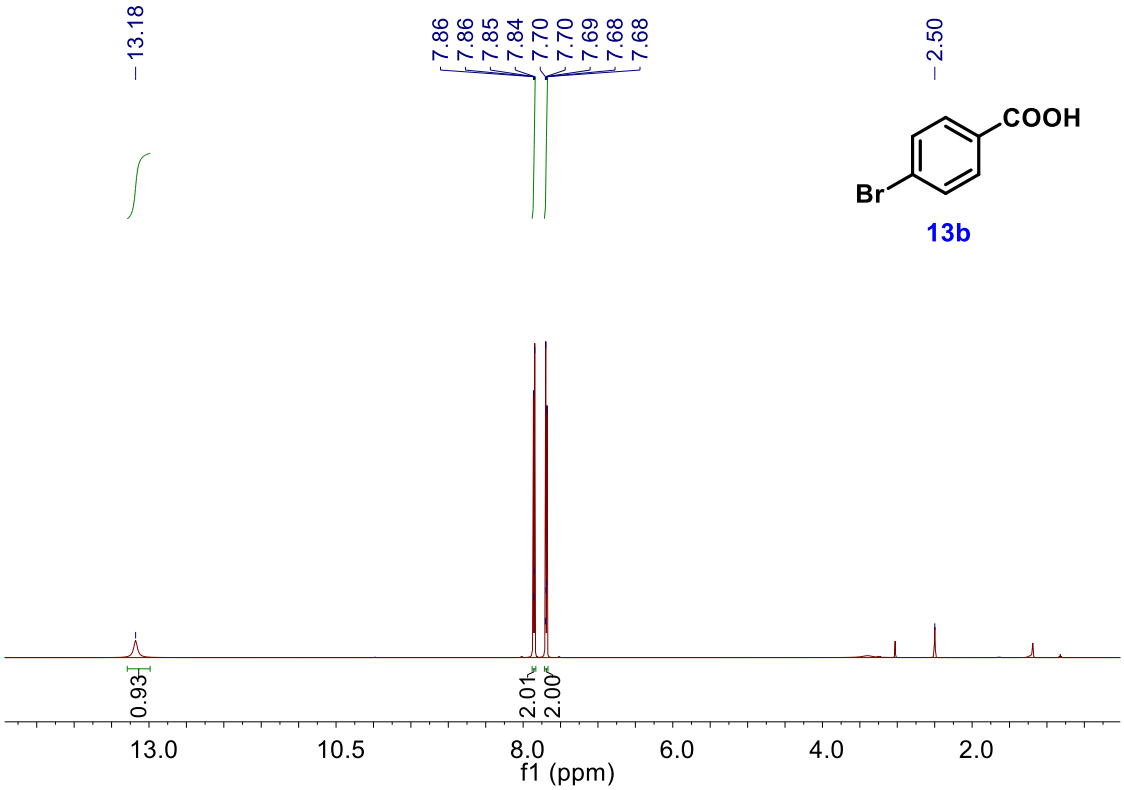
13.18
7.86
7.86
7.85
7.84
7.70
7.70
7.69
7.68
7.68
2.50
COOH
Br
13b
0.93
2.01
2.00
13.0
10.5
8.0
6.0
4.0
2.0
f1 (ppm)

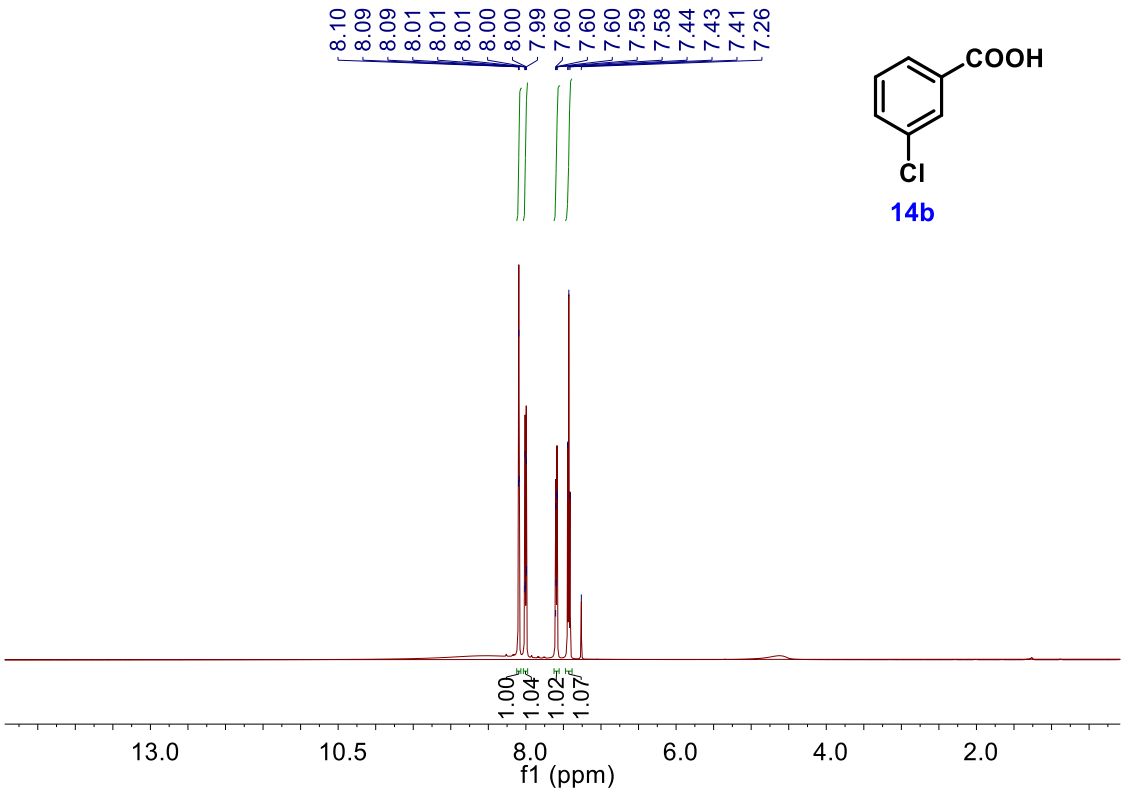
8.10
8.09
8.09
8.01
8.01
8.01
8.00
8.00
7.99
7.60
7.60
7.60
7.59
7.58
7.44
7.43
7.41
7.26
COOH
Cl
14b
1.00
1.04
1.02
1.07
13.0
10.5
8.0
6.0
4.0
2.0
f1 (ppm)

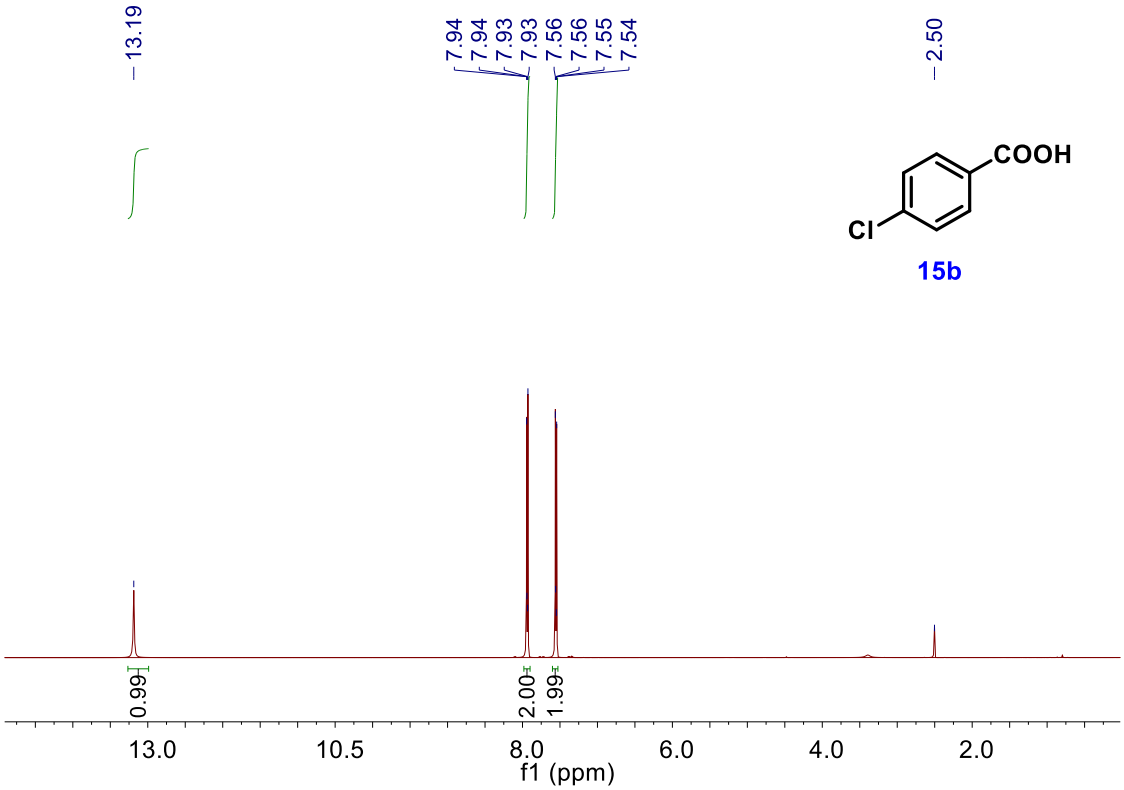
13.19
7.94
7.94
7.93
7.93
7.56
7.56
7.55
7.54
2.50
COOH
Cl
15b
0.99
2.00
1.99
13.0
10.5
8.0
6.0
4.0
2.0
f1 (ppm)